Journal of Applied Polymer Science

Stabilized electrospinning of heat stimuli/*in situ* crosslinkable nanofibers and their self-same nanocomposites

Kaan Bilge, Ayça Ürkmez, Eren Şimşek,* Melih Papila
Sabancı University, Materials Science and Engineering, Advanced Composites and Polymer Processing Laboratory, Tuzla, Istanbul, 34956, Turkey
*Presently at Quantag Nanotechnologies, Urla Izmir, Turkey
Correspondence to: M. Papila (E-mail: mpapila@sabanciuniv.edu)

ABSTRACT: We present a strategy for stabilizing the morphological integrity of electrospun polymeric nanofibers by heat stimuli *in situ* crosslinking. Amorphous polymer nanofibers, such as polystyrene (PS) and its co-polymers tend to lose their fiber morphology during processing at temperatures above their glass transition temperature (T_g) typically bound to happen in nanocomposite/structural composite applications. As an answer to this problem, incorporation of the crosslinking agents, phthalic anhydride (PA) and tributylamine (TBA), into the electrospinning polymer solution functionalized by glycidylmethacrylate (GMA) copolymerization, namely P(St-*co*-GMA), is demonstrated. Despite the presence of the crosslinker molecules, the electrospinning polymer solution is stable and its viscosity remains unaffected below 60 °C. Crosslinking reaction stands-by and can be thermally stimulated during post-processing of the electrospun P(St-*co*-GMA)/PA-TBA fiber mat at intermediate temperatures (below the T_g). This strategy enables the preservation of the nanofiber morphology during subsequent high temperature processing. The crosslinking event leads to an increase in T_g of the base polymer by 30 °C depending on degree of crosslinking. Crosslinked nanofibers are able to maintain their nanofibrous morphology above the T_g and upon exposure to organic solvents. *In situ* crosslinking in epoxy matrix is also reported as an example of high temperature demanding application/processing. Finally, a self-same fibrous nanocomposite is demonstrated by dual electrospinning of P(St-*co*-GMA) and stabilized P(St-*co*-GMA)/PA-TBA, forming an intermingled nanofibrous mat, followed by a heating cycle. The product is a composite of crosslinked P(St-*co*-GMA)/PA-TBA fibers fused by P(St-*co*-GMA) matrix. © 2016 Wiley Periodicals, Inc. J. Appl. Polym. Sci. **2016**, *133*, 44090.

KEYWORDS: crosslinking; electrospinning; glass transition; morphology

Received 28 January 2016; accepted 13 June 2016
DOI: 10.1002/app.44090

INTRODUCTION

Thanks to versatility of electrospinning and tailorable properties of its products for a wide range of applications, the research efforts on nanofibrous structures have consistently increased over the years. One of the promising fields of application is their usage as reinforcement materials in nanocomposites[1–7] and structural composites.[8–29] Morphology,[30,31] compatible chemistry,[1,32,33] and high surface area of preferably polymeric nanofiber mats are crucial for the anticipated performance in such applications.[34] Comprehension of the proposed material choices, limits, and their adaptation within conventional engineering processes should also be established for the coherent nanofiber based solutions. For instance, a relevant property especially in the case of highly amorphous polymers, is the glass transition temperature (T_g) as processing above which (likely with the composite/nanocomposite thermal processing cycles) can lead to distortion of the nanofibrous structure and morphology.

Potential solution to this problem is to facilitate chemical crosslinking of the polymer. Crosslinking can be induced to readily available electrospun polymeric nanofibers by exposing them to the corresponding crosslinking medium.[1,35,36] Such an *ex situ* implementation is arguably the conventional and direct way to achieve the crosslinked fibers. The major drawback of this method is that it causes permanent changes in chemistry and morphology of the nanofibrous structures prior to a subsequent application/integration step, e.g., their use as interlayers in the laminated composites.[2,8,10] Alternatively, *in situ* crosslinking methodology is relatively new bulk crosslinking technique. The term "*in situ*" comes from the fact that ingredients for the crosslinking are readily available "*in*" the base polymeric solution during electrospinning process.[37–42] The initiation of the

Table I. Electrospinnability of Different Polymer Solutions with Different Initiator Ratio, Crosslinking Agent Ratio, and Solution Concentration under Fixed Electrospinning Conditions

Initiator ratio (TBA/polymer by weight)	Solution concentration (polymer/DMF by weight)	Crosslinking agent ratio (R) (PA/GMA functional group ratio)	Nanofiber formation	Electrospinnability time (reason if = 0)
0.1%	10%	1	N	0 (Bead formation due to low solution viscosity)
		2	N	
		5	N	
		10	N	
	15%	1	Y	> 4 days
		2	Y	> 4 days
		5	Y	> 4 days
		10	Y	> 4 days
	20%	1	Y	< 2 h
		2	Y	< 1 h
		5	N	0 (Pre-mature crosslinking)
		10	N	0 (Pre-mature crosslinking)
	30% [1,8,32,33]	1	N	0 (Pre-mature crosslinking)
		2	N	
		5	N	
		10	N	
0.2%	All combinations	All combinations	N	0 (Pre-mature crosslinking)

crosslinking reaction is sought "*on-site*" by an external source of energy or stimuli (heat, UV light, etc.). To the best of our knowledge, main problem for the proposed *in situ* crosslinking methods in the literature is that they either require extra instrumentation or the continuous/stable electrospinning time is limited[42,43] due to increasing solution viscosity in the presence of crosslinking agents.

Present work offers a unique *in situ* crosslinking mechanism, which stands by at the room/regular operating temperature or lower and allows the continuous electrospinning from the polymer solutions. The crosslinking mechanism is activated by a designed heat stimuli so that electrospun nanofibers can keep the pristine morphological characteristics at elevated temperature uses/applications. Hence it is both possible to incorporate amorphous nanofibrous reinforcement into conventional raw composite materials (such as resin film and prepregs) at room temperature and then follow required processes (e.g., curing of epoxy) at elevated temperatures without the loss of nanofibrous morphology.

Efficiency of this method is exemplified in the use of highly amorphous polystyrene (PS), which was firstly functionalized by glycidylmethacrylate (GMA) copolymerization. The choice was made due to the fact that the fibrous network/mat is likely to lose the morphology when further processed above its T_g. The effect of the temperature increase on the nano-structure of P(St-*co*-GMA) nanofibers is shown by scanning electron microscopy (SEM) analyses of samples treated beyond the polymer T_g (around 100 °C). To circumvent the unwanted morphological changes, addition of an anhydride chemical crosslinking agent, phthalic anhydride (PA), and an appropriate tertiary amine catalyst, tributylamine (TBA), are herein considered. Continuously processable and yet heat stimuli-crosslinkable P(St-*co*-GMA) electrospun nanofibers were produced. Chemical crosslinking reaction onset temperature was found to be 60 °C, that is sufficiently far below the polymer T_g, as suggested in different epoxy/anhydride/tertiary amine crosslinking studies.[19–22] Any crosslinking reaction at the room temperature that can easily hinder consistent electrospinning due to an increase in solution viscosity is avoided. The stoichiometric ratio (R), PA volume with respect to the available epoxide rings in GMA groups, is tuned for maximum crosslinking and minimum morphological change above the T_g. Crosslinking characteristics and efficiency is measured by Fourier transform infrared spectroscopy (FTIR) and swelling tests. In addition, a systematic investigation of the temperature–morphology relation is presented by calorimetric and scanning electron microscopy (SEM) analyses.

The implementation and potential of the *in situ* crosslinking mechanism was demonstrated in two case studies. In the first

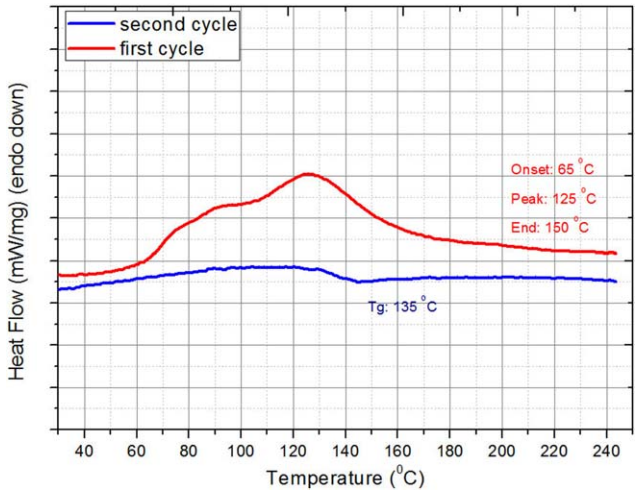

Figure 1. Preliminary two subsequent cycled DSC analysis for stabilized (SC)-P(St-*co*-GMA)/PA-TBA nanofibers with R = 2. [Color figure can be viewed in the online issue, which is available at wileyonlinelibrary.com.]

demonstration, heat stimuli crosslinkable nanofibers were introduced onto high temperature curing epoxy surfaces. The last demonstration was done by the manufacturing of self-same composites of un-crosslinked and *in situ* crosslinkable nanofibers by dual electrospinning.

EXPERIMENTAL

Copolymer Synthesis and Crosslinking Agents

The purified monomers of styrene (St) and glycidylmethacrylate (GMA), solvents dimethylformamide and methanol, and initiator azobisisobutyronitrile (AIBN) were purchased from Aldrich Chemical Co (Milwaukee, WI, USA). Free radical solution polymerization technique was used for copolymer P(St-*co*-GMA) synthesis. Styrene and GMA (by mole fractions m = 0.9 styrene and n = 0.1 GMA) were mixed at the round bottom reaction flask contained in an ice bath. Dimetylformamide (DMF) was then added into reaction flask with a 3:2 volume proportion solvent to monomer. The initiator AIBN was then added into monomer solvent mix and the reaction flask flushed with nitrogen.

The tube containing the dissolved monomers was then kept for 5 days in the constant temperature bath at 65 °C for the polymerization reaction. Finally, the polymer solution was poured out drop wise into a beaker containing methanol and the methanol/polymer mixture was filtered and dried in a vacuum oven at 60 °C for 1 day. The synthesized P(St-*co*-GMA) copolymer structure was determined by proton magnetic resonance spectroscopy (^{1}H-NMR). Molecular weights and polydispersities (PDI) were measured by a gel permeation chromatography (GPC) system and the molecular weight recorded as 220,000 g/mole with 1.54 PDI. As for the *in situ* crosslinking mechanism, the polymer solution recipe incorporates PA (phthalic anhydride) and an appropriate tertiary amine catalyst, TBA (tributylamine), purchased from Sigma Aldrich.

Electrospinning

In the framework for developing heat-stimuli *in situ* crosslinking mechanism, we also aimed to optimize the process and material parameters so that the electrospinning is continuous and forming bead-free nanofibers. Associated screening study was further discussed in the results section.

Execution of typical electrospinning procedure used throughout this work can be summarized as follows: (1) electrical charge (via Gamma high voltage ES 30P-20 W) was applied to polymer solutions contained in 2 mL syringe, which has an alligator clip attached to the blunt stainless steel syringe needle (diameter 300 μm). (2) The grounded collector covered with aluminum foil and a syringe pump (NewEra NE-1000 Syringe Pump) was used. (3) The applied voltage, solution flow rate, and tip to collector distance were set at 15 kV, 0.4 mL/h, and 10 cm, respectively, during the electrospinning. In the absence of crosslinker agents, the electrospinning parameters were chosen as reported in our previous works[1,8,32,33] (see Table I) where the applied voltage was 10 kV and polymer solution concentration was 30 wt %.

Thermal Characterization

The thermal properties of reference P(St-*co*-GMA) nanofibers along with stabilized P(St-*co*-GMA)/PA-TBA (prior to a heating scheme-SC, crosslinking stands by) and crosslinked P(St-*co*-GMA)/PA-TBA (posterior to the heating scheme-C) nanofibers were characterized with differential scanning calorimetric analyzer (Netzsch DSC 204). An initial study aiming to determine onset and peak temperatures of the crosslinking reaction was performed on the stabilized (SC)-P(St-*co*-GMA)/PA-TBA nanofibers with R = 2. The sample as received was analyzed by differential scanning calorimetry (DSC) as such the heat stimuli crosslinking reaction was triggered during the thermal scan in N_2 environment. Figure 1 shows the reaction graphic for P(St-*co*-GMA)/PA-TBA nanofibers (R = 2). The first heating cycle (upper curve) demonstrate that the exothermic reaction was

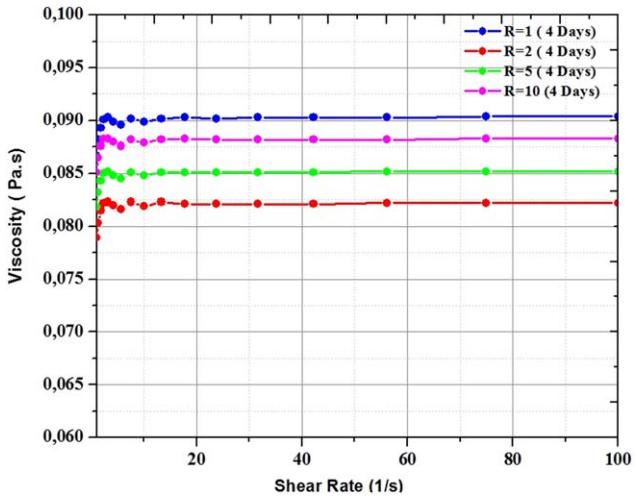

Figure 2. Preliminary viscosity vs. shear rate measurements for stabilized P(St-*co*-GMA)/PA-TBA nanofibers with R = 1, 2, 5, and 10. [Color figure can be viewed in the online issue, which is available at wileyonlinelibrary.com.]

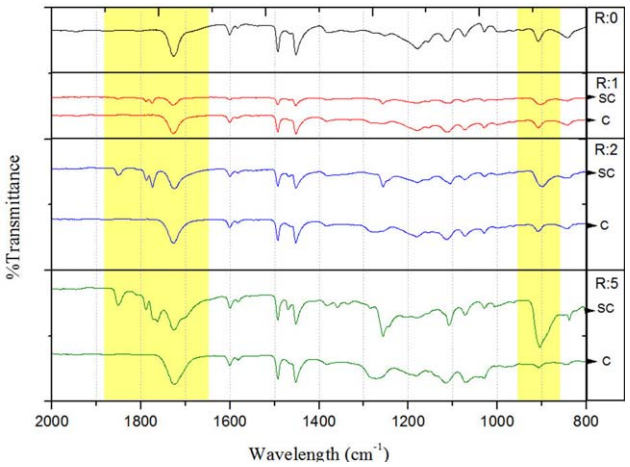

Figure 3. FTIR spectrum of P(St-*co*-GMA) (R:0), stabilized (SC), and crosslinked (C) P(St-*co*-GMA)/PA-TBA nanofibers. Each boxed out row includes stabilized (above) and crosslinked (below) nanofibers' spectrum pairs for an identical PA/Epoxide ring ratio marked at the right column of the graph. Shaded areas involve characteristic bands of the system. [Color figure can be viewed in the online issue, which is available at wileyonlinelibrary.com.]

acquired and the onset, peak, and end temperatures are 65 °C, 125 °C, and 150 °C, respectively. The second thermal cycle (lower curve) resulted in neither an exothermic nor endothermic reaction, it only revealed glass transition temperature (T_g: 135 °C). According to these characteristics, the crosslinking reaction occurs exothermically, subsequent cycle shows after a heating cycle there is not an exothermic reaction pattern therefore it can be concluded that the crosslinking reaction was completed.

This preliminary study showed that by the proposed crosslinking strategy we are able to crosslink P(St-*co*-GMA) nanofibers far below their T_g around 100 °C[1] (Figure 1). Note that, this characterization may not precisely reflect the thermal nature of the reaction in a real life application such as curing of polymeric composites since the overall reaction is not carried out in an inert gas ambient in contrast to DSC.

By referring to the observed onset and peak temperatures, P(St-*co*-GMA)/PA-TBA nanofibers were also crosslinked during a post heat treatment in an oven after electrospinning. The heat cycle was 2 h at 90 °C (just below polymer T_g to prevent morphological changes), and ramping up to 150 °C (above T_g) at 2 °C/min heating rate to dwell for 1 h at 150 °C. Crosslinked (C)-P(St-*co*-GMA)/PA-TBA nanofibers were then studied by DSC within a single heat cycle. Glass transition temperatures for different samples with R= 1, 2, 5, and 10 are reported.

Viscosity Measurements

Viscosity of the stabilized (SC)-P(St-*co*-GMA) polymer solution were determined via Anton Paar MCR302 rheometry with a shear rate control of 1–100 s^{-1} through a gap size of 0.208 mm.

Spectroscopic Characterization

The structures of stabilized (SC)- and crosslinked (C)-P(St-*co*-GMA)/PA-TBA nanofibers were characterized by Attenuated Total Reflection-Fourier transform infrared spectroscopy (ATR-FTIR). Analyses were performed with Thermo Scientific iS10 FTIR Spectrometer in the mid-infrared 4,000 cm^{-1} to 550 cm^{-1}.

Swelling Tests

The degree of crosslinking was determined by sol–gel analysis. Crosslinked (C)-P(St-*co*-GMA)/PA-TBA fibers were put into an aggressive solvent (DMF) effective on the base system P(St-*co*-GMA) and kept soaked for 72 h at room temperature. The swollen fibers were then cleaned with DMF and de-ionized water, which was followed by drying step in a vacuum oven at 70 °C. Crosslinking ratio is determined by measuring the gel fraction available in the specimens as follows:

$$\%\ \text{gel fraction} = 100 - [((m_i - m_f)/m_i) * 100]$$

where m_i and m_f corresponds to the initial mass and the dried mass of the sample, respectively.

Microscopic Characterization

The morphologies of stabilized (SC) P(St-*co*-GMA)/PA-TBA and crosslinked (C) P(St-*co*-GMA)/PA-TBA electrospun mats were compared. Scanning electron microscope. SEM LEO 1530VP was utilized employing secondary electron detector and in-lens detector at 2–5 kV after coating the specimens with Au–Pd for better electrical conduction. The fiber diameter analyses were carried out using ImageJ software.

RESULTS AND DISCUSSION

Electrospinning Process Parameters for Continuous and Bead Free Crosslinkable Nanofibers

In presence of the reaction initiator and crosslinking agent, it is essential to avoid any pre-mature crosslinking reaction, which can obstruct the electrospinning process. Therefore, we performed a preliminary screening study (see Table I) to determine correct amounts of these agents so that the polymer solution is continuously electrospinnable without any viscosity problems at fixed process parameters.

Table I suggests that the excessive catalyst TBA/polymer ratio in electrospinning may not be tolerated by tuning the overall solution concentration. With the addition of 0.2 wt % TBA, the polymer solution suffered from pre-mature crosslinking as such the electrospinning process was not applicable regardless of the solution concentration. Hence, the first decision was to decrease its set value to nominal 0.1 wt %. More practically, the amount of TBA corresponds to a single drop of TBA from a Pasteur pipette. The effect of the crosslinking agent (PA) amount was monitored in reference to the molar ratio of available active sites (epoxide ring) of P(St-*co*-GMA) in the solution. Four PA/Epoxide ring molar ratios, R, at 1, 2, 5, and 10 were investigated. For instance, R = 5 means that the mole number of PA added to P(St-*co*-GMA)/DMF solution is five times more than the mole number of available epoxide rings. In accordance with the PA ratio, the solution concentration was also tuned. In our previously reported studies on P(St-*co*-GMA),[1,8,32,33] the solution concentration was fixed at 30% resulting in stable nanofiber formation. However, in the presence of PA and TBA we were not able perform electrospinning continuously due to increased polymer viscosity and pre-mature crosslinking at room temperature depending on the choice of R. Hence, the

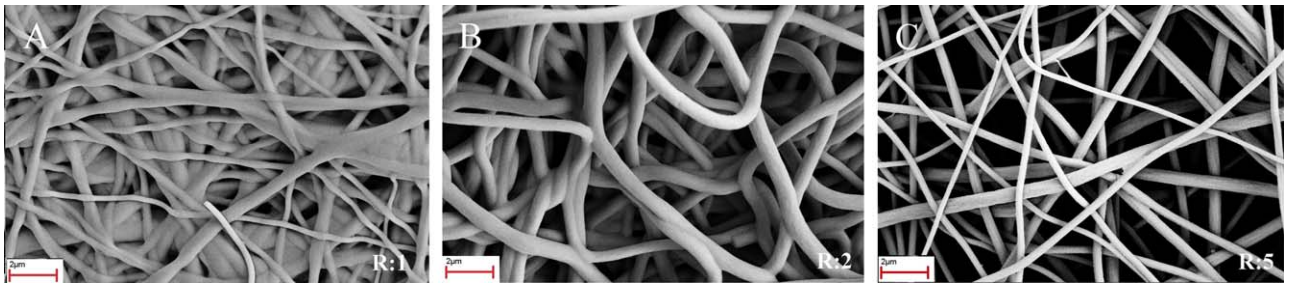

Figure 4. SEM micrographs of P(St-*co*-GMA)/PA-TBA nanofibers with PA/GMA ratios R:1(a), R:2 (b), and R:5 (c) after immersion in DMF 72 h. [Color figure can be viewed in the online issue, which is available at wileyonlinelibrary.com.]

Table II. Gel Fraction, Glass Transition Temperature, and Average Fiber Diameter Values for Cases Considered in the Study

PA/GMA molar ratio	Gel fraction (%)	Glass transition temperature (T_g)	As spun average fiber diameter (nm)	Above T_g average fiber diameter (nm)
R=0 (un-crosslinked)	—	98 ± 4	450 ± 40	—
R=1	95	103 ± 9	270 ±65	320 ± 150
R=2	97.7	111 ± 8	250 ± 80	310 ± 105
R=5	98.3	128 ± 4	320 ± 100	310 ± 90

solution viscosity was scanned in the solution concentration range of 10–30 wt %. At the lower end, the continuous nanofiber formation was not accomplished despite no pre-mature crosslinking. Instead polymeric beads were formed. However, when the solution concentration was increased to 15% the stable nanofiber formation was attainable and no-premature crosslinking was observed due to presence of TBA and PA (amounts given in Table I). The electrospinning process at room temperature was continuous without any unfavorable changes in the fibrous jet formation until we stopped monitoring after straight 10 h. These observations were supported by rheology measurements carried out on the polymer solutions after 4 days of storage at room temperature without any stirring application (shaded rows in Table I, i.e., polymer solutions with 15% solution concentration with R = 1, 2, 5, and 10). Figure 2 shows the corresponding shear rate vs. viscosity measurements. As a result of these measurements, it can be deducted that the crosslinking at room temperature was standing by and there was not any viscosity change in the polymer solutions with increasing shear rates.

Nature and Degree of Crosslinking

Proposed heat-stimulated reaction for the crosslinking of P(St-*co*-GMA)/PA-TBA is reported by Papila *et al.*[44]

FTIR measurements were performed on samples of electrospun P(St-*co*-GMA)/PA-TBA nanofibers before and after the heat treatment. The samples were, so called here, stabilized (SC) and crosslinked (C), respectively, along with the reference P(St-*co*-GMA) nanofibers. The results confirmed the anticipated crosslinking and its dependence to the ratio R. Figure 3 shows the FTIR spectra for nanofibers indicating the effect of various R ratios. The characteristic bands of the reaction are at 1,851 cm^{-1} and 1,787 cm^{-1} [$\nu_{s,(C=O)}$ and $\nu_{as,(C=O)}$ of the anhydride ring], 902 cm^{-1} [$\nu_{s,(C-O)}$ overlapping epoxide (907 cm^{-1}) and anhydride (902 cm^{-1}) absorptions]. The intensities of these characteristic peaks decrease due to the reacting species during the crosslinking (SC vs. C). However, they increase with the increasing PA/Epoxide ring ratio R from 1 to 5 among the stabilized nanofibers (not heat treated).

Moreover, the characteristic epoxide ring stretching at 902 cm^{-1} remains distinguishable after the crosslinking reaction due to the remaining oxirane ring moiety. However, these moieties decay with the increasing PA/Epoxide ring ratio due to larger extent of the crosslinking. Additionally, intensity of the peak at 1,727 cm^{-1} [$\nu_{s,(C=O)}$ ester] increases with the formation of the ester groups, which is also a proof of the anticipated crosslinking.[45–47]

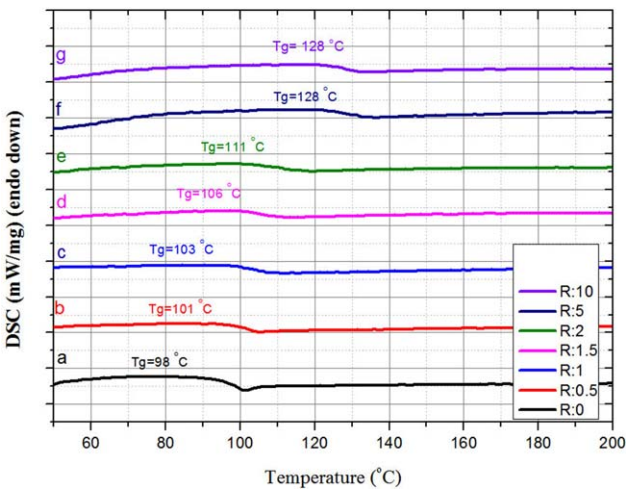

Figure 5. DSC curves of un-crosslinked P(St-*co*-GMA) (a, R:0) and crosslinked (b–g) P(St-*co*-GMA)/PA-TBA nanofibers. PA to epoxide ring ratio (R) for b–g 0.5, 1, 1.5, 2, 5, and 10, respectively. [Color figure can be viewed in the online issue, which is available at wileyonlinelibrary.com.]

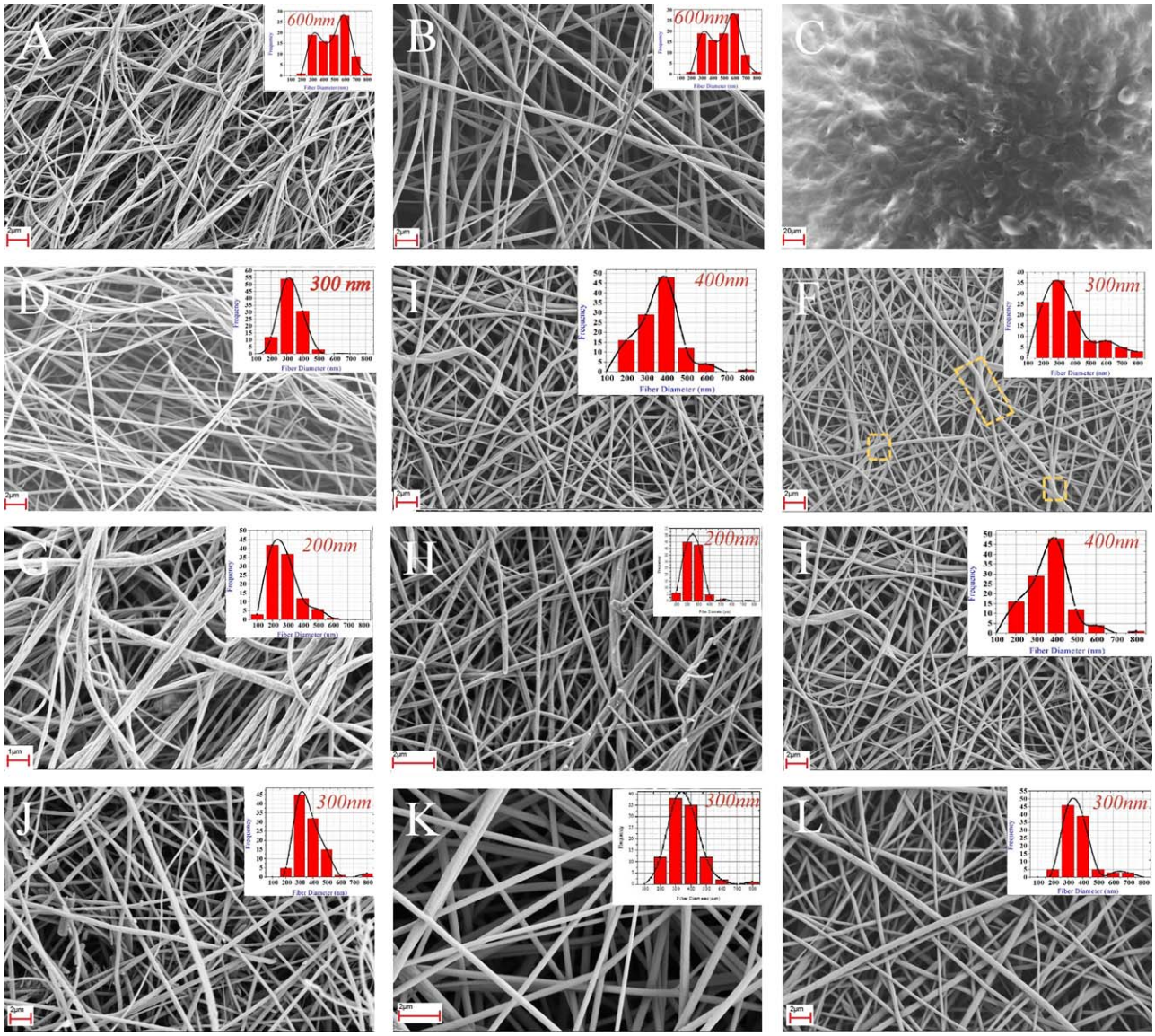

Figure 6. SEM micrographs of electrospun fibers. Each raw includes SEM images of the fibers prior to heat treatment (left image column), after the heat treatment at 90°C 2 h (center image column), post heat treatment at 150°C (right image column). Scale bars: 2 μm for a,b,d–l; and 20 μm for c. Nanofiber diameter distribution charts reports fiber diameters ranging from 100 to 800 nm where each bar is of a hundred nm bin width. Numbers over the distribution graphs notes the fiber diameter of the highest count in the respective image analysis. Yellow dashed circle/ellipse: fusing/branching of the fibers onto the other. [Color figure can be viewed in the online issue, which is available at wileyonlinelibrary.com.]

Swelling test results also confirmed that the chemical crosslinking is achievable with applied heating scheme. They showed that the gel fraction for crosslinked nanofibers increased from 95% to 98.3% (Table II) with increasing R ratio whereas the reference P(St-*co*-GMA) nanofibers were completely soluble in DMF solutions. Swelling associated morphological features/changes are shown by SEM images (Figure 4) after storing the nanofibers in DMF solvent. They suggest that the nanofibrous microstructure becomes stable and is preserved as the degree of crosslinking increases. It can be noted that the crosslinked nanofibers, which are with a PA/GMA ratio R = 5, are arguably unaffected by the solvent exposure. Transformation into the ribbon-like or notably swelled fibrous morphology was avoided unlike in cases of R = 1 and R = 2, respectively, for which the swelling with surface erosion[11] is considered to be the root-cause.

Glass Transition: Overcoming the Barrier

The DSC analyses of the crosslinked P(St-*co*-GMA)/PA-TBA (after the heating scheme applied) and reference P(St-*co*-GMA) nanofibers were carried out in order to identify the effects of the crosslinking on the thermal transitions (Figure 5). Glass transition temperature was raised from 98 °C (reference by P(St-*co*-GMA) sample) up to 128 °C with the increasing PA/Epoxide ring ratio R. This is attributed to the decreasing flexibility of polymer chains with the increasing extent of the crosslinking. Beyond R = 5, the crosslinker amount can be considered saturated in regard to the resultant crosslinking density and associated thermal stability, that is the crosslinking ratio was found to

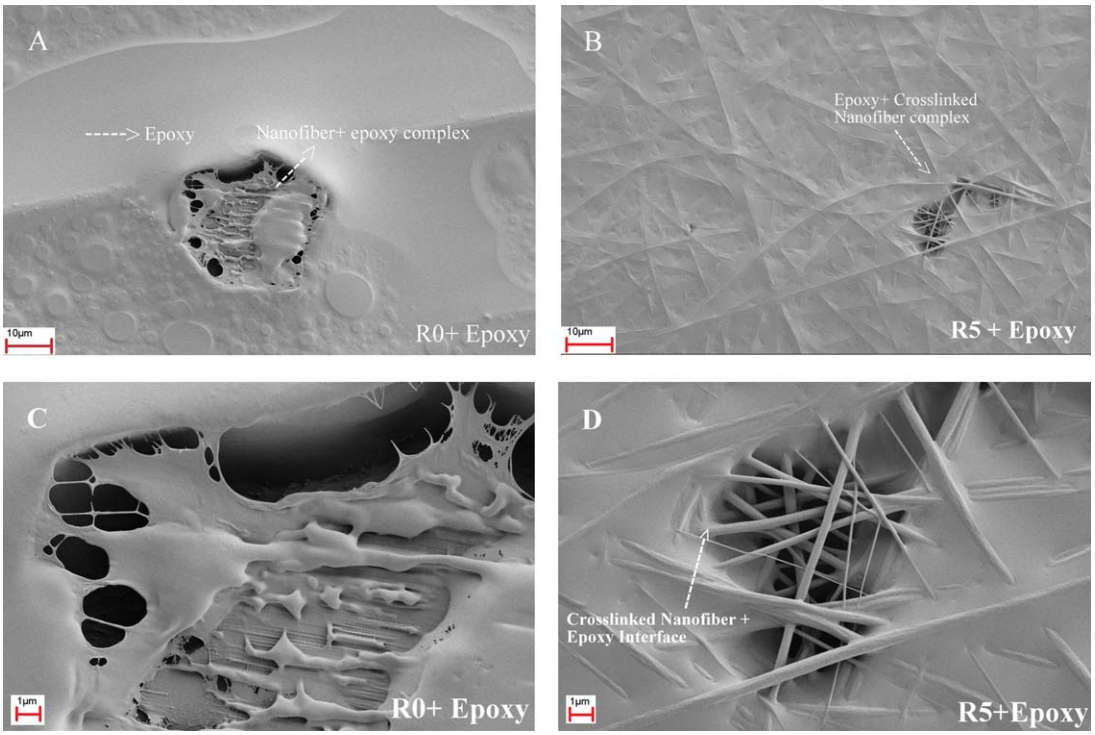

Figure 7. SEM micrographs of P(St-*co*-GMA) (a,c) and P(St-*co*-GMA)/PA-TBA (b,d) on cured epoxy surfaces. [Color figure can be viewed in the online issue, which is available at wileyonlinelibrary.com.]

converge and remain unchanged despite increase of PA. It is also important to point out that with the applied heating cycle on the nanofibers crosslinking reactions were complete as such no distinguishable exothermic reaction peak was observed in the individual DSC runs.

Fiber morphologies of the reference P(St-*co*-GMA), stabilized (SC) P(St-*co*-GMA)/PA-TBA, and crosslinked (C) P(St-*co*-GMA)/PA-TBA nanofibers were examined for the selected PA/epoxide ring ratios R. The SEM images of the nanofibers prior and posterior to the heat treatments are given in Figure 6. Fiber diameter distribution charts are also attached onto the images. Recall that (Electrospinning section) applied voltage for no-crosslinker case (R = 0) was 10 kV in compliance with our earlier work,[8,32,33] whereas 15 kV was found to work better for homogenous fiber formations in the cases of the crosslinking agent (R = 1, 2, and 5: less spread in the fiber diameter can be noted in Figure 6(d,g), 300–400 nm). Despite the increased voltage, no disruptive jet instability was observed. The morphological change along with the preserved continuity of the jet can be attributed to the increase in the electrostatic repulsive forces in the existence of crosslinker agents.[48,49]

Substantiating our motivation for this work, un-crosslinked/reference P(St-*co*-GMA) nanofibers were found losing their form/morphology when processed above their glass transition temperature $T_g \approx 100\,^{\circ}C$ [Figure 6(c)]. This is attributed to highly amorphous nature of P(St-*co*-GMA) nanofibers and associated softening effect above the T_g. We conclude that unconstrained mobility of the polymer chains promoted interactions between the individual fibers ultimately causing the loss of fibrous structure. On the contrary, in the cases of P(St-*co*-GMA)/PA-TBA nanofibers with R = 1, 2, and 5 [Figure 6(f,i,l), respectively] the fibrous morphologies were preserved beyond the T_g as a consequence of the heat stimuli/*in situ* crosslinking as anticipated. Furthermore, fiber diameter distribution along with the

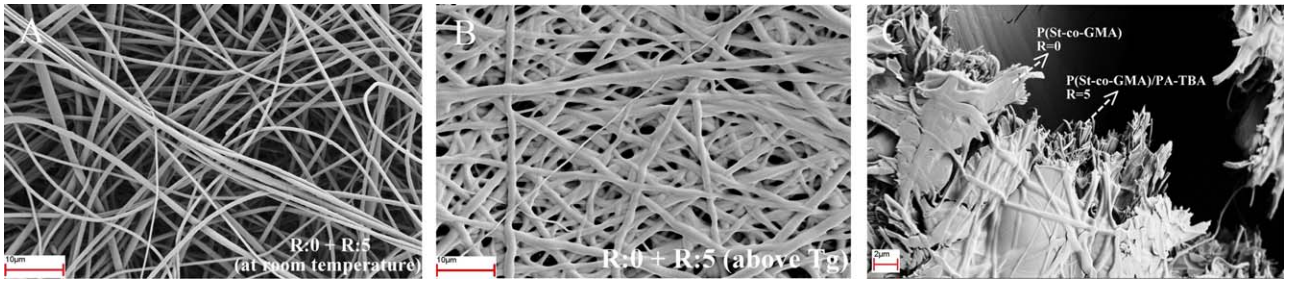

Figure 8. SEM micrographs of dual electrospun P(St-*co*-GMA) (R:0) and stabilized P(St-*co*-GMA)/PA-TBA (R:5) nanofibers at room temperature (a), at 150 °C (b), and cross-sectional view at 150 °C (c). [Color figure can be viewed in the online issue, which is available at wileyonlinelibrary.com.]

morphological changes suggest the transition into more discrete/uniform nanofibers is correlated with the level of intramolecular crosslinking[43] [Figure 6(d,e) for R = 1, Figure 6(g,h) for R = 2, and Figure 6(j,k) for R = 5]. It is worth noting the existence of somewhat flattened fibers and fusing/branching at the fiber interactions in R = 1 and 2 cases [dashed line enclosures on Figure 6(h,k)] as opposed to R = 5 case [Figure 6(l)], which was considered herein the maximum crosslinking configuration. It can also be claimed that the proposed heat stimulated/*in situ* crosslink mechanism enforced nanofibers to shrink volumetrically, hence the diameter distributions were likely to converge into a narrower band as sampled and analyzed from the images.

An Application Example of High Temperature Processing: *In Situ* Crosslinking of Nanofibers during Epoxy Matrix Cure Cycle

The heat-stimuli crosslinkable nanofibers can be used in composite materials as reinforcing and toughening agents. High performance epoxy resin systems demand processing at elevated temperature typically above the T_g of many amorphous polymers. In this specific demonstration, heat stimuli crosslinkable P(St-*co*-GMA)/PA-TBA (with R = 5) and pristine/reference P(St-*co*-GMA) nanofibers were electrospun onto carbon/epoxy prepreg surfaces (Aldila Composites, 34–700 (24k)-AR2527). The nanofiber coated epoxy matrix prepreg plies were cured at 150 °C for 2 h, which is above the T_g of P(St-*co*-GMA) nanofiber (Figure 5). Heat-stimuli crosslinking methodology was adopted as an intermediate hold-time of 120 min at 90 °C, to treat the nanofibers on the prepreg ply before its ultimate cure at 150 °C. As it can be seen in Figure 7(a,c) the nanofibrous morphology of the reference P(St-*co*-GMA) nanofibers was totally lost, similar to Figure 6(b). However, P(St-*co*-GMA)/PA-TBA nanofibers were exposed to the proposed *in situ* crosslinking process effectively and kept their nanofibrous formation while being embedded into epoxy matrix [Figure 7(b)]. Furthermore, they formed an effective interface with the epoxy matrix [Figure 7(d)], which is in line with our previously reported composite application studies.[1,8,32,33]

Self-Same Nanofibrous Composites

The effect of crosslinker ratio *R* and associated morphological changes above the T_g can be taken advantage of to facilitate what we called a "self-same nanofibrous composites". To demonstrate this, we propose dual electrospinning of the reference (backbone) polymer P(St-*co*-GMA) (R = 0) together with the stabilized crosslinkable P(St-*co*-GMA)/PA-TBA (R = 5) nanofibers. The two polymer solutions were electrospun simultaneously from different syringes onto the same collector. Resultant intermingled fibrous web of the two polymeric nanofibers was obtained [Figure 8(a)]. When this initially intermingled web was heat processed above the T_g condition, morphological changes of the two different fibers of their own occurred in concert as described in the previous section. That is, stabilized nanofibers were to crosslink and shrink, and backbone nanofibers were to lose their fibrous morphology by spreading.

Clear change in the fibrous structure is shown in Figure 8(b) where crosslinked nanofibers can be spotted. The morphology after the heat cycle is unique and different from the ones reported in Figure 6. Observations in Figures 6–8 suggest that the un-crosslinked backbone polymer P(St-*co*-GMA) wraps/fuses onto the crosslinked fibers creating a self-same nanofibrous composite film. In other words, un-crosslinked nanofibers processed above the T_g interacted with the crosslinkable fibers and hereby acted as a self-same matrix material for the crosslinked nanofibers. Cross-sectional view presented as Figure 8(c) also confirmed that with the application of the proposed processing, it is possible to create a polymeric film reinforced by nanofibers just by heating. We believe that this concept is worth of further considerations by a dedicated work.

CONCLUSIONS

Heat-stimulated crosslinking capability was introduced into amorphous P(St-*co*-GMA) nanofibers, by the addition of phthalic anhydride (PA) as the crosslinking agent and tributylamine (TBA) as the initiator. Despite the mixing of the crosslinker agents into the solution, crosslinking was successfully suppressed at room temperature, allowing continuous electrospinning without any adverse effect on the polymer solution viscosity. The crosslinking reaction was found to be initiated at around 60 °C. Electrospun nanofibers with different PA amounts were crosslinked by the application of thermal cycle at intermediate temperatures of ~90 °C (*i.e.*, just below T_g). Crosslinking at the highest capacity was sought, when the PA/epoxide ring (GMA) molar ratio was varied from 1 to 5. A proposed reaction route was validated by FTIR analyses, where the consumption of PA and available epoxide rings in GMA was observed. Swelling tests suggested that the gel fraction in crosslinked nanofibers maximized with the increasing PA amount up to molar ratio of 5. At the maximum crosslinking ratio, P(St-*co*-GMA)/PA-TBA nanofibers completely preserved their pristine nanofibrous morphology after 3 days of exposure to DMF solvent. The DSC analyses suggested that the T_g of the crosslinked nanofibers increased with the degree of crosslinking, by up to 30 °C. Note that the glass transition temperature T_g may also be an important limit, as exceeding it may induce substantial changes in the nanofibrous structure/morphology. Un-crosslinked P(St-*co*-GMA) nanofibrous morphology and network degraded above their T_g, whereas the crosslinked P(St-*co*-GMA)/PA-TBA nanofibers, especially the ones with $R = 5$, were able to maintain their nanofibrous morphology intact. A similar outcome was observed when R = 5 P(St-*co*-GMA)/PA-TBA nanofibers were processed *in situ* at 150 °C accommodating the cure of the epoxy matrix. The fibrous morphology was contained and the P(St-*co*-GMA)/PA-TBA nanofibers were effectively embedded into the epoxy matrix.

Lastly, the form-loose effect of an above-the-T_g process on the P(St-*co*-GMA) fibers was proposed as a strategy in the manufacturing of what we call the self-same nanocomposites. Un-crosslinked (R = 0) and stabilized crosslinkable (R = 5) nanofibers of P(St-*co*-GMA) backbone polymer were electrospun together by dual electrospinning. An intermingled nanofibrous structure were formed. The two types of fibers interacted upon a subsequent processing above the T_g reforming into a nanocomposite fibrous network, where the un-crosslinked P(St-

co-GMA) appears to wrap/fuse around the self-crosslinkable P(St-*co*-GMA)/PA-TBA nanofibers.

ACKNOWLEDGMENTS

Graduate student and material supports from TUBITAK Grant number 213M542.

REFERENCES

1. Ozden, E.; Menceloglu, Y. Z.; Papila, M. *ACS Appl. Mater. Interfaces* **2010**, *2*, 1788.
2. Kim, J. S.; Reneker, D. H. *Polym. Compos.* **1999**, *20*, 124.
3. Bergshoef, M. M.; Vansco, G. *J. Adv. Mater.* **1999**, *11*, 1362.
4. Romo-Uribe, A.; Arizmendi, L.; Romero-Guzman, M. E.; Sepulveda-Guzman, S.; Cruz-Silva, R. *ACS Appl. Mater. Interfaces* **2009**, *1*, 2502.
5. Chen, L. S.; Huang, Z. M.; Dong, G. H.; He, C. L.; Liu, L.; Hu, Y. Y. *Polym. Compos.* **2009**, *30*, 239.
6. Nepalli, R.; Marega, C.; Marigo, A.; Bajgaj, M. P.; Kim, H. Y.; Causin, V. *Eur. Polym. J.* **2010**, *46*, 968.
7. Lee, J.-R.; Park, S.-J.; Seo, M.-K.; Park, J.-M. *Mater. Res. Soc. Symp. Proc.* **2004**, NN5.11.
8. Bilge, K.; Ozden-Yenigun, E.; Simsek, E.; Menceloglu, Y. Z.; Papila, M. *Compos. Sci. Technol.* **2012**, *72*, 1639.
9. Dzenis, Y. *Science* **2008**, *319*, 419.
10. Dzenis, Y.; Reneker, D. H. U.S. Pat. 626533 (**2001**).
11. Sihn, S.; Kim, R. Y.; Huh, W.; Lee, K. -H.; Roy, A. K. *Compos. Sci. Technol.* **2008**, *68*, 673.
12. Liu, L.; Huang, Z. -M.; He, C.; Han, X. *Mater. Sci. Eng. A* **2006**, *435*, 309.
13. Liu, L.; Huang, Z. M.; Xu, G. Y.; Liang, Y. M.; Dong, G. H. *Polym. Compos.* **2008**, *29*, 285.
14. Lee, S. -H.; Lee, J. -H.; Cheong, S. -K.; Noguchi, H. A. *J. Mater. Process. Technol.* **2008**, *207*, 21.
15. Lee, S. -H.; Noguchi, H.; Kim, Y. -B.; Cheong, S. -K. *J. Compos. Mater.* **2002**, *36*, 2153.
16. Palazetti, R.; Zuchelli, A.; Gualandi, C.; Focarete, M.; Donati, L.; Minak, G. *Compos. Struct.* **2012**, *94*, 571.
17. Magniez, K.; Chaffraix, T.; Fox, B. *Materials* **2011**, *4*, 1967.
18. Zhang, J.; Lin, T.; Wang, X. *Compos. Sci. Technol.* **2010**, *70*, 1660.
19. Zhang, J.; Lin, T.; Wang, C. H. *Compos. Sci. Technol.* **2012**, *72*, 256.
20. Bortz, D. R.; Merino, C.; Martin-Gullon, I. *Composites A* **2011**, *42*, 1584.
21. Nash, N. H.; Young, T. M.; McGrail, P. T.; Stanley, W. F. *Mater. Des.* **2015**, *85*, 582.
22. Liu, L.; Zhang, H.; Zhou, Y. *Compos. Struct.* **2014**, *111*, 436.
23. Li, P.; Liu, D.; Zhu, B.; Li, B.; Jia, X.; Wang, L.; Li, G.; Yang, X. *Composites A* **2015**, *68*, 72.
24. Ary Subagia, I. D. G.; Jiang, Z.; Tijing, L. D.; Kim, Y.; Kim, C. S.; Lim, J. K. *Fibers Polym.* **2014**, *15*, 1295.
25. Daelemans, L.; Van Der Heijden, S.; De Baere, I.; Rahier, H.; Van Paepegem, W.; De Clerck, K. *Compos. Sci. Technol.* **2015**, *117*, 244.
26. Van Der Heijden, S.; Daelemans, L.; Schoenmaker, B. D.; De Baere, I.; Rahier, H.; Van Paepegem, W.; De Clerck, K. *Compos. Sci. Technol.* **2014**, *104*, 66.
27. Saghafi, H.; Palazetti, R.; Zuchelli, A.; Minak, G. *J. Reinf. Plast. Compos.* **2015**, *34*, 907.
28. Beckermann, G. W.; Pickering, K. L. *Composites A* **2015**, *72*, 11.
29. Palazetti, R. *J. Compos. Mater.* **2014**, *49*, 3407.
30. Zheng, J.; He, A.; Li, j.; Xu, J.; Han, C. C. *Polymer* **2006**, *47*, 7095.
31. Yordem, O.; Papila, M.; Menceloglu, Y. Z. *Mater. Des.* **2008**, *29*, 34.
32. Ozden-Yenigun, E.; Menceloglu, Y. Z.; Papila, M. *Appl. Mater. Interfaces* **2012**, *4*, 777.
33. Bilge, K.; Venkataraman, S.; Menceloglu, Y. Z.; Papila, M. *Composites A* **2014**, *58*, 73.
34. Huang, Z.-M.; Zhang, Y.-Z.; Koataki, M.; Ramakrishna, S. *Compos. Sci. Technol.* **2003**, *63*, 2223.
35. Dai, T.; Ebert, K. *J. Appl. Polym. Sci.* **2012**, *126*, 136.
36. Peresin, M. S.; Vesterinen, A. H.; Habibi, Y.; Johansson, L. S.; Pawlak, J. J.; Nevzorov, A. A. *J. Appl. Polym. Sci.* **2014**, *131*, DOI: 10.1002/app.40334.
37. Gupta, P.; Trenor, S. R.; Long, T. E.; Wilkes, G. L. *Macromolecules* **2004**, *37*, 9211.
38. Kim, S. H.; Kim, S. -H.; Nair, S.; Moore, E. *Macromolecules* **2005**, *38*, 3719.
39. Ji, Y.; Ghosh, K.; Li, B.; Sokolov, J. C.; Clark, R. A.; Rafailovich, M. H. *Macromol. Biosci.* **2006**, *6*, 811.
40. Stone, S. A.; Gosavi, P.; Athauda, T. J.; Ozer, R. R. *Mater. Lett.* **2013**, *112*, 32.
41. Liu, H.; Zhen, M.; Wu, R. *Hydrogel Nanofibers Chem. Phys.* **2007**, *208*, 874.
42. Acatay, K.; Simsek, E.; Ow-Yang, C.; Menceloglu, Y. Z. *Angew. Chem. Int. Edit* **2004**, *43*, 5210.
43. Tang, C.; Saquing, C. D.; Harding, J. R.; Khan, S. *Macromolecules* **2010**, *43*, 630.
44. Papila, M.; Bilge, K.; Şimşek, E.; Ürkmez, A.; Menceloğlu, Y.; Ozden-Yeniguün, E. Patent Corporation Treaty (PCT) Applied Patent Ref No: PCT/TR2015/000227.
45. Luo, X.; Zheng, S.; Ma, D. *J. Polym. Sci.* **1995**, *13*, 144.
46. Romao, B. M. V.; Diniz, M. F.; Azevedo, M. F. P.; Lourenco, V. L.; Pardini, L. C.; Dutra, R. C. L. *Polímeros* **2006**, *13*, 144.
47. Antoon, M. K.; Koenig, J. L. *J. Polym. Sci. Polym. Chem. Ed.* **1981**, *19*, 549.
48. Huan, S.; Liu, G.; Han, G.; Cheng, W.; Fu, Z.; Wu, Q.; Wang, Q. *Materials* **2015**, *8*, 2718.
49. Yuan, X.; Zhang, Y.; Dong, C.; Sheng, J. *Polym. Int.* **2004**, *53*, 1704.